Published as: *Neuron*. 2014 July 2; 83(1): 93–103.

Linx mediates inter-axonal interactions and formation of the internal capsule

Kenji Mandai[1,2,*], **Dorothy V. Reimert**[1], and **David D. Ginty**[1,3,*]

[1]The Solomon H. Snyder Department of Neuroscience, Howard Hughes Medical Institute, The Johns Hopkins University School of Medicine, 725 North Wolfe Street, Baltimore, MD, 21205, USA

[2]Department of Biochemistry and Molecular Biology, Kobe University Graduate School of Medicine, 7-5-1 Kusunoki-cho, Chuo-ku, Kobe, Hyogo 650-0017, Japan

[3]The Department of Neurobiology, Howard Hughes Medical Institute, Harvard Medical School, 220 Longwood Avenue, Armenise 435, Boston, MA 02115, USA

Summary

During the development of forebrain connectivity, ascending thalamocortical and descending corticofugal axons first intermingle at the pallial-subpallial boundary to form the internal capsule (IC). However, the identity of molecular cues that guide these axons remains largely unknown. Here, we show that the transmembrane protein Linx is robustly expressed in the prethalamus and lateral ganglionic eminence-derived corridor and on corticofugal axons, but not on thalamocortical axons, and that mice with a null mutation of *Linx* exhibit a complete absence of the IC. Moreover, regional inactivation of *Linx* either in the prethalamus and LGE or in the neocortex leads to a failure of IC formation. Furthermore, Linx binds to thalamocortical projections and it promotes outgrowth of thalamic axons. Thus, Linx guides the extension of thalamocortical axons in the ventral forebrain and subsequently, it mediates reciprocal interactions between thalamocortical and corticofugal axons to form the IC.

Introduction

The internal capsule (IC) is a major brain tract comprised of thalamocortical and corticofugal projections that reciprocally connect the neocortex and subcortical structures. How ascending thalamocortical and descending corticofugal projections are guided to their appropriate cortical and subcortical targets, respectively, is a major unanswered question. In the mouse, ascending thalamocortical axons reach the diencephalic-telencephalic boundary (DTB) by embryonic day (E) 12.5 (López-Bendito and Molnár, 2003). Upon reaching the DTB, these axons change their trajectory, extend through the ventral forebrain and, by

*Correspondence should be addressed to K.M. (mandai@med.kobe-u.ac.jp) and D.D.G. (david_ginty@hms.harvard.edu).

E13.5, reach the pallial-subpallial boundary (PSPB). Guidepost cells of the prethalamus and corridor cells derived from the lateral ganglionic eminence (LGE) serve to direct thalamocortical projections through the DTB, into the medial ganglionic eminence and towards the PSPB (López-Bendito et al., 2006; Métin and Godement, 1996). On the other hand, descending corticofugal axons emanating from deep layers of the neocortex reach the PSPB at ∼E13.5 when they transiently pause prior to invasion of the subpallium. This waiting period is regulated by Sema3E/PlexinD1 signaling (Deck et al., 2013). At the PSPB, thalamocortical and corticofugal axons intermingle and then extend in close proximity to each other and in opposite directions *en route* to cortical and subcortical targets, respectively (Hevner et al., 2002; McConnell et al., 1989; Molnár et al., 1998a). According to the "handshake hypothesis" (Blakemore and Molnár, 1990), thalamocortical and corticofugal axons associate at the PSPB (Molnár et al., 1998a; Molnar et al., 1998b), and this association between ascending and descending axons serves to guide their distal projections, beyond the PSPB to appropriate target regions. Indeed, recent findings indicate that descending corticofugal axons are required to guide ascending thalamic axons across the PSPB (Chen et al., 2012; Molnár et al., 2012). The identity of cues that mediate interactions (i.e. the handshake) between thalamocortical and corticofugal axons at the PSPB and that guide ascending and descending axonal projections across this boundary have been elusive (Molnár et al., 2012).

Linx is a *LIG* gene family transmembrane protein originally described as a mediator of axonal extension, branching, and guidance of somatosensory and spinal motor neurons (Mandai et al., 2009). Here, we demonstrate that Linx is robustly expressed on corticofugal axons, but not on thalamocortical axons, and that mice with a null mutation of *Linx* exhibit a complete absence of the IC, although layer V cortical neurons and thalamic neurons are otherwise intact. Moreover, regional inactivation of Linx either in the prethalamus and LGE or in the neocortex leads to a failure of IC formation. Furthermore, Linx binds to thalamocortical projections and promotes their outgrowth. Thus, Linx guides the extension of thalamocortical axons in the ventral forebrain and it mediates reciprocal interactions between thalamocortical and corticofugal axons at the PSPB and guidance and extension of all ascending and descending projections of the mammalian neocortex.

Results

Linx expression in the developing brain

To determine whether Linx controls axonal projections in the mammalian brain, we first assessed the spatial and temporal patterns of Linx expression in brains of embryonic and neonatal mice. Linx protein is detected in the developing brain as early as E11.5 and is most abundant during late gestation, while levels are relatively low in the adult brain (Figure 1A). At E14.5, Linx protein is robustly expressed in the cerebral cortex, prethalamus (nomenclature described elsewhere (Puelles and Rubenstein, 2003)), LGE, and the LGE-derived corridor that penetrates the medial ganglionic eminence and provides a permissive substrate for extension of thalamocortical axons (Figure 1B) (Bielle et al., 2011). On the other hand, Linx is undetectable in the thalamus and globus pallidus at this stage. *In situ* hybridization for *Linx* mRNA confirms these expression patterns (Figure 1B). At postnatal

day (P) 0, Linx protein is most highly associated with the IC (Figure 1C). We also assessed the cellular pattern of Linx expression in the developing cortex utilizing a *Linx* knockin allele (*Linx*^{tEGFP}) in which the coding determinants of a tau-enhanced green fluorescent protein (EGFP) fusion protein were introduced into the *Linx* locus (Mandai et al., 2009). At E12.5, *Linx* is expressed in virtually all Ctip2 (alias, Bcl11b)-positive cortical projection neurons in layer V of the pallium (Arlotta et al., 2005) (Figure 1D). At E13.5, *Linx* is expressed in the pretectum but not in the thalamus, which expresses Foxp2 (Ferland et al., 2003; Suzuki-Hirano et al., 2011) (Figure 1E). Additionally, analysis of older embryos revealed that *Linx* is highly expressed in corticofugal neurons in deep cortical layers including layers V and VI and the subplate, as well as neurons of the marginal zone (Figures 1F, 3C and 3D). Thus, although absent from axons of thalamocortical neurons, Linx is highly expressed both in the prethalamus and within the corridor of the developing striatum through which thalamocortical axons project. Linx is also highly expressed on the majority of L1-positive axons of the cortex, with the exception of those in the deepest cortical layer (Figure 1F). Thus, Linx is highly expressed on most axons of the deep cortical neurons that give rise to corticofugal projections, which associate via the handshake with Linx^{-} thalamocortical axons at the PSPB. This pattern of Linx expression, together with its previously defined role as a mediator of axonal growth and guidance in the peripheral nervous system (Mandai et al., 2009), prompted us to examine its role in both the initial trajectory of corticofugal axons and as a mediator of reciprocal interactions between corticofugal and thalamocortical axons.

Requirement of Linx for formation of the internal capsule

To assess the involvement of Linx during establishment of forebrain neuronal circuits, and of corticofugal and thalamocortical projections in particular, we analyzed brains of E18.5 *Linx* null mice. Strikingly, *Linx* mutant embryos exhibit a complete absence of the IC, and thalamocortical projections that normally form the ascending component of the IC are markedly aberrant in these mutant embryos (Figures 2A and 2B). Remnants of the descending component of the IC are tangled within the striatum of mutant mice (Figure 2B). In control animals, projections emanating from the thalamus cross the DTB and extend into the pallium. In contrast, essentially all thalamic projections in *Linx* null mice fail to penetrate the DTB and are instead misrouted into the ventral midbrain where they terminate entangled within the hypothalamus (Figures 2A and 2B). This dramatic fiber tract projection defect is also readily observed at E14.5 (Figure S2A). To further visualize the thalamocortical and corticofugal projection defects in *Linx* mutants, we performed lipophilic dye-tracing experiments on E18.5 control and *Linx* null embryos. In control heterozygous embryos, DiI crystals placed in either the thalamus or somatosensory cortex revealed the typical robust axonal tracts that project via the IC to connect these structures (Figures 2C and 2D). In contrast, DiI crystals placed in thalami of *Linx* null mice confirmed that anterogradely labeled thalamocortical axons do not cross the DTB and instead project aberrantly into the hypothalamus (Figure 2C). Moreover, DiI crystals placed within the somatosensory cortex of *Linx* mutants showed that anterogradely labeled corticofugal axons fail to project into the subpallium (Figure 2D). Similarly, DiI crystals placed within the visual cortex of *Linx* mutants showed that anterogradely labeled corticofugal axons fail to project into the subpallium (Figure S2B). These observations indicate that Linx is essential

for the formation of both ascending thalamocortical projections and descending corticofugal projections, thus explaining the complete absence of the IC in *Linx* mutant mice. On the other hand, the corpus callosum, another major brain fiber tract emanating from the cortex, appears normally formed in *Linx* mutants (Figure S2C).

Why do thalamocortical and corticofugal projections of the IC fail to develop in *Linx* mutant mice? We began to address this question by examining thalamocortical axons and their relationship to the LGE-derived corridor, which guides thalamocortical projections through the subpallium *en route* to the cortex (López-Bendito et al., 2006). At E13.5, thalamocortical axons of *Linx* mutants, labeled by anti-Neurofilament immunostaining, have already bypassed the corridor and misprojected to the hypothalamus (Figures 3A and S3A). Foxp2 immunostaining indicates that thalamic neurons appear normally specified and localized in *Linx* mutants (Figure 3B). Therefore, thalamocortical axon misprojections may come about because of deficient corridor-derived signals or, more fundamentally, the corridor itself may fail to form. Thus, the integrity of the corridor was assessed using Islet1 and Ebf1 immunostaining of E13.5 embryos. Brain sections depicting the caudal region of the IC revealed that the medial tip of the corridor is improperly formed in mutant embryos (Figures 3A and S3A). In contrast, the rostral region of the corridor as well as the medial ganglionic eminence and globus pallidus are fully formed and normally organized (Figures S3B and S3C). Although Linx is not expressed in thalamocortical neurons themselves, it is highly expressed in a zone immediately adjacent to the DTB through which thalamocortical axons extend (Figure S3D). EGFP expression in control $Linx^{+/tEGFP}$ embryos was observed in the ventral forebrain near the DTB at E12.5, a time when thalamocortical projections descend through the prethalamus and are about to cross the DTB. The pattern of EGFP expression in the ventral forebrain of *Linx* null ($Linx^{tEGFP/tEGFP}$) embryos was similar to that seen in control heterozygous embryos, indicating that tissue organization is unchanged in the mutants. These findings suggest that Linx expressed in cells adjacent to the DTB is crucial for navigation or elongation of thalamocortical projections through the DTB, and possibly for formation of the most caudal region of the corridor.

We next tested the possibility that an absence of deep layer cortical pyramidal neurons, which give rise to corticofugal projections, is a primary defect in *Linx* mutants. This appears not to be the case because layer V pyramidal neurons, labeled with Ctip2, are present, albeit in slightly increased numbers, and properly located in the cortex of P0 *Linx* null embryos (Figures 3C and 3E). Moreover, subplate neurons and layer VI neurons, labeled with Zfpm2, are present in normal numbers and location in the mutant cortex (Figures 3D and 3E). Therefore, we next sought to determine the time and location along the cortical pyramidal neuron axonal trajectory in which Linx is required for corticofugal axonal pathfinding. Fortunately, the $Linx^{tEGFP}$ knockin allele strongly labels corticofugal projections with EGFP, allowing visualization of these descending projections in both $Linx^{tEGFP}$ heterozygous control and homozygous null mutants. Since thalamocortical neurons do not express *Linx*, the ascending axons of the IC are not labeled by EGFP in $Linx^{tEGFP}$ mice (Figure 1B). Using $Linx^{tEGFP}$ mice, we observed that axons of deep layer cortical pyramidal neurons extend to within close proximity to the PSPB at E13.5 and that the morphology of these fibers and their proximity to the PSPB are indistinguishable in heterozygous control

and homozygous null littermate embryos at this age (Figure 3F). However, several days later, at E18.5, after corticofugal projections of heterozygous control mice have intermingled with thalamocortical fibers at the PSPB and extended across this boundary to form the IC within the subpallium, these same projections in *Linx* mutant littermates have stalled at the PSPB. Thus, Linx is dispensable for the formation of deep layer cortical neurons and their initial trajectory towards the PSPB, but it is essential for corticofugal axon penetration of the PSPB and extension within the subpallium. Prior findings indicate that thalamocortical projections traverse the PSPB in close association with descending corticofugal fibers, and that this association is required for corticofugal axons to cross the PSPB and enter the subpallium *en route* to subcortical targets (López-Bendito and Molnár, 2003). Therefore, our observations suggest that the ventral misrouting of thalamocortical axons, and their failure to project to the PSPB, results in lack of thalamocortical and corticofugal axon association, and thus stalling of corticofugal projections at the PSPB.

Since Linx is robustly expressed along the path through which IC axons extend, and since thalamocortical projections do not express Linx, we hypothesized that Linx expressed on corridor cells binds to proteins expressed on thalamocortical axons to promote their guidance or extension across the DTB. We further hypothesized that, at a later stage, Linx expressed on corticofugal axons serves a similar function at the PSPB, promoting or allowing thalamocortical axons to extend along corticofugal fibers into the cortex and, reciprocally, enabling corticofugal axons to enter the subpallium and project towards subcortical targets. To begin to test this model, we first developed an *in situ* binding assay using an alkaline-phosphatase tagged ectodomain of Linx (AP-Linx) as a probe to visualize the localization of Linx binding sites in the developing forebrain (Figure 4A). Remarkably, the AP-Linx ligand bound mainly to thalamocortical projections in coronal brain sections of E14.5 embryos. The same specimens were co-immunostained with anti-Linx and anti-Neurofilament (Figure 4B) to visualize the relationship between Linx-expressing cells of the LGE-derived corridor and Linx binding sites on thalamocortical axons. This analysis revealed that thalamocortical projections, which express Linx binding sites, pass through a pipe-like structure surrounded by cells that robustly express Linx. The intimate relationship between Linx-expressing cells of the LGE-derived corridor and thalamocortical axons expressing Linx binding sites suggests a direct effect of Linx on thalamocortical axon growth or guidance. Therefore, we next asked whether Linx presented directly to thalamocortical neurons promotes axonal extension. For this, dissociated thalamic neurons from E13.5 mice were co-cultured with control HEK293T cells or HEK293T cells engineered to express Linx, and then thalamic neuron axon length was measured (Figure 4C). Thalamic neurons grown on Linx-expressing 293T cells displayed axons that are nearly two-fold longer than those grown on mock-transfected 293T cells. Taken together, these findings support a model in which Linx expressed on LGE-derived corridor cells adjacent to the DTB of the ventral forebrain binds to a receptor located on thalamocortical axons to promote their extension through the corridor. Moreover, Linx expressed on axons of layer V, VI, and VIb (subplate) neurons may serve a similar function in both the ventral forebrain and at the PSPB to promote thalamocortical axons to associate with, and extend along corticofugal fibers into the neocortex.

Requirement of Linx in the dorsal and ventral forebrains for formation of the IC

To test this model and to determine the cell type requirement of Linx function, we generated a conditional *Linx* allele (*Linx*^{flox}) that allows Cre recombinase-mediated, region-specific ablation of *Linx* (Figure S4). To assess the role of *Linx* expressed in the prethalamus and LGE-derived corridor, we generated *Linx*$^{flox/tEGFP}$;*Dlx5/6*-Cre mice (Puelles and Rubenstein, 2003; Stenman et al., 2003) to ablate *Linx* in these brain structures and examined the formation of the IC at P0. The *Dlx5/6*-Cre-mediated region-specific inactivation of Linx was confirmed by Linx immunostaining (Figure 5A), which showed that Linx expression in the prethalamus and LGE is lost at E14.5 in *Linx*$^{flox/tEGFP}$;*Dlx5/6*-Cre mice. Phenotypically, the IC is disorganized in *Linx*$^{flox/tEGFP}$;*Dlx5/6*-Cre mice, although the rostral part of the tract is partially formed in these mutants (Figure 5B). In caudal sections, thalamic projections are dramatically misrouted into the ventral midbrain and tangled within the hypothalamus, similar to *Linx* null mice (see Figures 2A, 2B, and 2C). In addition, axons labeled with a neurofilament antibody are reduced in the neocortex of *Linx*$^{flox/tEGFP}$;*Dlx5/6*-Cre mice. DiI crystals placed in the somatosensory cortex or thalamus of *Linx*$^{flox/tEGFP}$; *Dlx5/6*-Cre mutant mice revealed a near complete absence of corticofugal and thalamocortical axons that cross the PSPB (Figures 5C and 5D). Thus, Linx expressed in *Dlx5/6*-positive cells of the prethalamus and/or LGE-derived corridor is required for thalamocortical axon pathfinding through the DTB, towards the neocortex, and across the PSPB.

We next tested the hypothesis that Linx on corticofugal axons mediates thalamocortical and corticofugal axon interactions, extension across the PSPB, and subsequent growth towards their respective cortical and subcortical targets. For this, we generated *Linx*$^{flox/tEGFP}$;*Emx1*-Cre mice (Gorski et al., 2002) to selectively inactivate *Linx* in embryonic projection neurons of the neocortex, but not in neurons of subcortical structures including the thalamus, prethalamus, and LGE-derived corridor. *Emx1*-Cre-mediated regional inactivation of Linx was confirmed by Linx immunostaining (Figure 6A). Indeed, Linx expression in the neocortex, but not the thalamus, prethalamus, or LGE-derived corridor, is lost in these mutants at E14.5. In *Linx*$^{flox/tEGFP}$;*Emx1*-Cre mutant mice, thalamocortical projections extend properly through the DTB and the IC is formed, although it is markedly hypoplastic (Figure 6B). Strikingly, the main trunk of the IC is devoid of corticofugal axons, as visualized using anti-EGFP. Furthermore, few if any corticofugal and thalamocortical axons have crossed the PSPB in *Linx*$^{flox/tEGFP}$;*Emx1*-Cre mutants (Figure 6C). To further visualize the precise location of the thalamocortical and corticofugal projection defects in *Linx*$^{flox/tEGFP}$;*Emx1*-Cre mutant mice, lipophilic dye-tracing experiments were performed. In control *Linx*$^{+/tEGFP}$;*Emx1*-Cre mice, DiI crystals placed in the somatosensory cortex indeed showed robust axonal tracts that project through the PSPB to connect the somatosensory cortex and the thalamus (Figure 6D). In contrast, DiI crystals placed in the somatosensory cortex of *Linx*$^{flox/tEGFP}$;*Emx1*-Cre mutant mice revealed a near complete absence of corticofugal axons that cross the PSPB. Similarly, DiI crystals placed in the thalamus of *Linx*$^{flox/tEGFP}$;*Emx1*-Cre mutant mice showed an absence of thalamocortical axons that cross the PSPB (Figure 6E). These observations indicate that Linx expressed on corticofugal fibers emanating from deep layer neurons of the neocortex is required for reciprocal corticofugal and thalamocortical axonal interactions at the PSPB and extension of

both fiber bundles beyond the PSPB towards their subcortical and cortical targets, respectively.

We next asked whether the dramatic defects observed in *Linx* mutant mice are the result of a developmental delay or an absolute requirement of *Linx* for IC formation by examining postnatal brains of *Linx* conditional mutant mice. Remarkably, in contrast to *Linx* null mutants, which die at birth (Mandai et al., 2009), both $Linx^{flox/tEGFP}$;*Dlx5/6*-Cre and $Linx^{flox/tEGFP}$;*Emx1*-Cre mutant mice survive until three weeks of age. Then, during their fourth postnatal week, approximately 60% of $Linx^{flox/tEGFP}$;*Dlx5/6*-Cre mutants and 15% of $Linx^{flox/tEGFP}$;*Emx1*-Cre mutants die (Figure S4). At postnatal day 7 (P7), in $Linx^{flox/tEGFP}$; *Emx1*-Cre mutants, the pallium and the subpallium are almost completely disconnected and very few *Linx*-positive corticofugal axons were observed in the ventral forebrain (Figure 7A). Similarly, in $Linx^{flox/tEGFP}$; *Dlx5/6*-Cre mutants at P7, the pallium and the subpallium are nearly completely disconnected and a small number of *Linx*-positive corticofugal axons remain entangled within the ventral forebrain (Figure 7B). In the pons and medulla of the brainstem of P7 control $Linx^{+/tEGFP}$;*Emx1*-Cre mice, the corticospinal tract (CST) was visualized with PKCγ immunohistochemistry (Figure 7C). The CST also strongly expresses GFP in control mice. However, in P7 $Linx^{flox/tEGFP}$;*Emx1*-Cre mutants, as expected, the CST is completely absent. Likewise, in $Linx^{flox/tEGFP}$; *Dlx5/6*-Cre mutants at P7, few GFP-positive CST axons were observed extending into the pons and medulla. These findings indicate that the IC phenotype observed at embryonic stages in *Linx* mutants is not a consequence of a developmental delay, rather Linx expressed in *Emx1*-positive cortical projection neurons and in *Dlx5/6*-positive striatal neurons is required for formation of corticofugal projections, including those that extend into the spinal cord. Therefore, essentially all connections between pallial and subpallial structures are developmentally and permanently disconnected in *Linx*-deficient mice (Figures 2, 3F, 5C, 6D, 7, and S2B).

Discussion

The handshake model, proposed over 23 years ago (Blakemore and Molnár, 1990), provides a conceptual framework for understanding how cortical efferent and afferent projections interact at the PSPB and guide each other to their respective subcortical and cortical targets. On the other hand, thalamocortical axons, during an earlier stage of IC formation, are navigated through the ventral forebrain by cues derived from LGE-derived corridor cells (Leyva-Díaz and López-Bendito, 2013; López-Bendito et al., 2006). We report here the identification of an inter-axonal signaling mechanism that mediates the handshake interaction at the PSPB and thalamocortical and corticofugal axonal pathfinding in both the neocortex and ventral forebrain.

The transmembrane protein Linx was first described as being required for formation of sensory and motor projections in the periphery (Mandai et al., 2009). Here, we show that this transmembrane cue functions in two distinct locations to control thalamocortical and corticofugal axon navigation during forebrain development. First, Linx expressed on cells of the prethalamus and/or LGE-derived corridor supports extension of proximal thalamocortical axons across the DTB and through the LGE-derived corridor. A Linx binding partner, its putative receptor, is expressed on thalamocortical axons, and Linx

promotes thalamocortical axon extension *in vitro*. These observations support a model in which Linx expressed in cells located within, or in close proximity to, the DTB and corridor directly promotes growth and/or guidance of thalamocortical axons through the DTB. Mechanistically, prethalamic (PTh-Th) and telencephalic (VTel-Th) guidepost cells (Molnár et al., 2012) may be the critical sources of Linx that promote extension of thalamocortical axons *en route* to the neocortex. Thalamic axon guidance cues, which include slits, netrin-1, neuregulin-1, ephrins, EphB1/2, Sema3A, and Sema3F (Demyanenko et al., 2011; Dufour et al., 2003; López-Bendito et al., 2006; Métin et al., 1997; Robichaux et al., 2014; Wright et al., 2007), may cooperatively function with Linx to establish early thalamocortical projections through the DTB en route to the cortex. Linx may also modulate expression or availability of thalamic axon guidance cues.

Importantly, Linx functions at a second site along the trajectory of thalamocortical axons, the PSPB. Indeed, Linx expressed on corticofugal axons emanating from deep layer neurons of the neocortex, which first encounter thalamocortical axons at the PSPB, is necessary for extension of both thalamocortical axons and corticofugal axons through the PSPB and towards their final destinations within the cortex and subcortical targets, respectively. These findings indicate that Linx is a long-sought mediator of reciprocal thalamocortical and corticofugal axonal interactions (i.e. the handshake) and thus guidance and extension of all ascending and descending projections of the neocortex.

Several gene knockout mice exhibit defects in the IC, and Linx may interact directly or indirectly with the products of one or more of these genes to promote thalamocortical and corticofugal axonal pathfinding. IC defects are observed in mice lacking the transcription factors *Pax6*, *Mash1/Ascl1* and *Gbx2* and the transmembrane proteins *Fzd3*, *Pcdh10* and *Celsr3* (Hevner et al., 2002; Stoykova et al., 1996; Tuttle et al., 1999; Uemura et al., 2007; Wang et al., 2002; Zhou et al., 2008). In *Pax6*, *Fzd3*, *Pcdh10* and *Celsr3* mutant mice, corticofugal and thalamocortical projections are absent, while, in *Gbx2* mutant mice, these projections are absent or dramatically reduced. Whether any or all these genes function in the same cell types and at the same developmental stages as described here for *Linx* is at present unclear. Direct comparisons of the forebrain defects following regional inactivation of *Pax6*, *Mash1/Ascl1*, *Gbx2*, *Pcdh10*, *Fzd3*, *Celsr3* and *Linx*, and intercrosses that test for genetic interactions between these genes, may reveal novel signaling pathways involving *Linx* that function to control thalamocortical and corticofugal axonal pathfinding.

In summary, Linx is a key inter-axonal signal that mediates both thalamocortical axonal pathfinding within the ventral forebrain and thalamocortical and corticofugal handshake interactions at the PSPB. Future work will focus on identification of the Linx binding partner(s) expressed on thalamocortical axons and the mechanism by which Linx promotes extension of thalamocortical and corticofugal axons through the PSPB.

Experimental Procedures

Mouse lines, and the generation of mice harboring a conditional *Linx* allele

All animal procedures were approved by the Animal Care and Use Committee at the Johns Hopkins University School of Medicine or Kobe University Graduate School of Medicine.

The mouse lines used in this study, *Linx*^{tEGFP} (Mandai et al., 2009), *Dlx5/6*-Cre (Stenman et al., 2003), and *Emx1*-Cre (Gorski et al., 2002), were maintained on a C57BL/6 background. The day when a vaginal plug was observed is designated as E0.5.

To generate mice harboring the *Linx*^{flox} allele, an 11.2-kb fragment of *Linx* genomic DNA (an *AatII* site to a *ClaI* site) was inserted into pBluescript-DTA (Figure S3). This vector contains a cDNA encoding the diphtheria toxin A-fragment for negative selection of embryonic stem (ES) cells. For construction of the targeting vector, a recombineering-based method was used (Liu et al., 2003). One of the mini-targeting vectors was constructed with a PL452 vector providing a *lox*P site, and 2 homology arms generated by PCR with primer pairs, A and B, and C and D and a subcloned genomic DNA as a template. The other mini-targeting vector was constructed with a PL451 vector containing an *FRT-PGK-EM7-Neo-polyA-FRT-loxP* cassette, and 2 homology arms generated by PCR with primer pairs, E and F, and G and H and a subcloned genomic DNA as a template. Using the subcloned *Linx* genomic DNA in pBluescript-DTA and 2 mini-targeting vectors, the targeting vector was generated by recombineering. As a result, *lox*P sites were inserted between exon 2 and 3, and downstream of the stop codon in exon 3. Cre-mediated recombination results in deletion of the entire protein coding sequence of *Linx*. After electrotransformation of the targeting vector, 129/Sv ES cells harboring the targeted allele were selected for G418 resistance. Positive ES cell clones were identified by PCR. Karyotypically normal ES cells were injected into C57BL/6 blastocysts that were then introduced into pseudopregnant females to yield chimeric mice. Chimeric mice were bred with C57BL/6 mice to generate agouti heterozygous mice harboring the mutated allele (*Linx*$^{+/flox}$), and subsequently these mice were crossed with mice expressing FlpE recombinase in the germ cell lineage to excise the *PGK-EM7-Neo-pA* cassette. The *Linx*$^{+/flox}$ and wild-type alleles were identified by PCR using a primer pair, I and J. The PCR reaction consists of 2 min at 95°C followed by 38 cycles of 30 s at 95°C, 30 s at 57°C, and 25 s at 72°C. The primer pair yields a 271-bp band for the wild-type allele and a 376-bp band for the mutant allele. To eliminate Linx in excitatory neurons of the forebrain, conditional knockout mice were crossed with *Emx1-Cre* mice. Loss of Linx protein expression in the ventral forebrain, cerebellum, or pons was assessed by immunohistochemistry to confirm efficiency and specificity of recombination. The abovementioned primers are listed:

Primer A, 5′- AAGTCGACGCTAGGGGTTCGGTCTCAGAG-3′;

Primer B, 5′-TTGAATTCACTAGTCCTTATCTGGAACTGCCCCCT-3′;

Primer C, 5′-AAGGATCCGGATAGATGGGAGCTGGGG-3′;

Primer D, 5′-TTGCGGCCGCTGACTCTACCGTGCGTACC-3′;

Primer E, 5′-AAGTCGACCGTCCCTGCTGGTTATCG-3′;

Primer F, 5′-TTGAATTCTAGAGCAGGCCAGGCGTGCTG-3′;

Primer G, 5′-TAAGATCTCCACCTCCACCTTGGGTAC-3′;

Primer H, 5′ -TTGCGGCCGCGGTGAGAATAAAAATTAGC-3′;

Primer I, 5′-CGGCAACTACAGGCAGAC-3′; and

Primer J, 5′-GGAGGTAGGAGCCTGACTC-3′.

In situ hybridization, immunohistochemistry, immunocytochemistry, and axon-tracing experiments

For *in situ* hybridization, freshly frozen E14.5 embryos were embedded and sectioned at 20-μm thickness. Riboprobes were prepared with digoxigenin using a construct previously described (Mandai et al., 2009). Sections were incubated with approximately 1 μg/ml probe at 65°C overnight. Hybridized probes were detected with alkaline-phosphatase labeled anti-digoxigenin (Roche) followed by incubation with 4-nitro blue tetrazolium chloride (NBT) and 5-bromo-4-chloro-3-indolyl-phosphate, 4-toluidine salt (BCIP) (Roche).

For immunohistochemistry, tissues were freshly frozen or fixed with 4% ice-cold paraformaldehyde (PFA) followed by cryoprotection with 30% sucrose in phosphate-buffered saline (PBS). They were sectioned at 16-20-μm thickness after embedding in Tissue-Tek O.C.T. compound (Sakura). For Islet1, Neurofilament, and Nkx2.1 immunostaining, sections were boiled for 15 min in 10 mM sodium citrate buffer (pH 6.0) for antigen retrieval. For Ebf1, Zfpm2, and Foxp2 immunostaining, sections were incubated at 65°C for 20 min in HistoVT One™ (Nacalai) for antigen retrieval. Sections were permeabilized for 15 min with 0.3% Triton X-100 in PBS for Ctip2, Ebf1, Foxp2, Zfpm2, and L1 immunostaining or 0.15% Triton X-100 in PBS for all of the other immunostaining experiments. Sections were blocked by incubation with 1% bovine serum albumin in PBS for 20 min. Primary antibodies were diluted in blocking buffer and incubated on sections at 4°C overnight. The following antibodies were used: rabbit anti-mouse Linx (Mandai et al., 2009), rat anti-human Ctip2 (25B6) (Abcam, 1:500), rabbit anti-GFP (Molecular Probes, 1:1000), rat anti-GFP (GF090R) (Nacalai, 1:1000), rabbit anti-human Foxp2 (Abcam, 1:2000), rat ant-mouse L1 (324) (Millipore, 1:50), rabbit anti-mouse Zfpm2/FOG-2 (M-247) (Santa Cruz, 1:250), rabbit anti-mouse PKCγ (C-19) (Santa Cruz, 1:250), rabbit anti-mouse Ebf1 (Millipore, 1:1000), mouse anti-Nkx2.1/TTF-1 (8G7G3/1) (Dako, 1:50), mouse anti-rat Neurofilament (2H3) (Developmental Studies Hybridoma Bank, 1:20, culture supernatant), and rabbit anti-human Islet1 (Abcam, 1:500). Secondary antibody incubations were performed with Alexa Fluor-conjugated antibodies (Molecular Probes, 1:500) or biotinylated secondary antibodies, which were detected using the VECTASTAIN ABC system (Vector laboratories) followed by a horseradish peroxidase reaction with 3, 3′-diaminobenzidine (DAB). TO-PRO-3 iodide or 4′,6-Diamidino-2-Phenylindole, Dihydrochloride (DAPI) (Molecular Probes) were used for nuclear counterstain.

For immunocytochemistry, cells were fixed with 4% ice-cold PFA for 15 min and permeabilized using 0.15% Triton X-100 in PBS for 15 min, followed by incubation with 1% bovine serum albumin in PBS for 20 min for blocking. Cells were incubated in blocking buffer containing mouse class III β-tubulin (Tuj1) (Covance, 1:2000) antibody at 4°C overnight, followed by secondary antibody incubation.

For axon-tracing experiments, E18.5 or P0 brains were fixed in 4% PFA in PBS overnight. Small crystals (approximately 0.1-mm diameter) of 1,1′-dioctadecyl-3,3,3′,3′-tetramethylindocarbocyanine perchlorate (DiI; Molecular Probes) were inserted into either the thalamus or the somatosensory cortex after sagittal bisection of the brains using needles.

After insertion of crystals, the tissues were stored in 4% PFA in PBS at 37°C for 3 weeks, and then cut on a vibratome into 150 or 200-um sections. Sections were counterstained with Hoechst 33258 (Molecular Probes) or DAPI.

All images were captured using an Axioskop2 (Carl Zeiss) or a confocal imaging system (LSM 5 Pascal or LSM 510 Meta; Carl Zeiss).

In situ binding assay with alkaline-phosphatase tagged Linx on tissue sections

To prepare AP-Linx, a cDNA encoding the ectodomain of mouse Linx without its signal peptide (amino acids 20 to 590) was inserted into the XhoI and XbaI sites of the pAPtag-5 vector (GeneHunter). The AP-tagged ligand was prepared as described (Giger et al., 1998). *In situ* section binding assay was performed as described with modifications (Flanagan et al., 2000). In brief, freshly prepared frozen E14.5 embryos were sectioned at 20-um thickness and fixed in methanol at −20°C for 8 min. The sections were incubated with AP ligand (AP-Linx, or AP alone as a control), which had been pre-incubated at 4°C for 2 h with anti-Myc to cluster the ligands. After washing the sections with 0.1% Triton X-100 in TBSM (20 mM Tris-HCl pH7.4, 150 mM NaCl, 4 mM $MgCl_2$), they were incubated in TBSM at 65°C for 2.5 h to inactivate endogenous alkaline phosphatase. The color reaction was performed with NBT and BCIP to visualize ligand-binding sites on tissue sections.

Immunoblotting experiments

Heads of E11.5 embryos and forebrains for other time points were homogenized in a buffer (20 mM Tris-HCl at pH7.4, 150 mM NaCl, and 1 mM EDTA) containing protease inhibitors (20 ng/ml leupeptin, 1 ng/ml pepstatin A, and 1 mM PMSF (Roche)), and then centrifuged at 900 × *g* for 10 min. The supernatants (40 μg of protein each) were subjected to SDS-PAGE followed by immunoblotting using the Linx antibody (Mandai et al., 2009).

Primary thalamic neuronal cultures

The dorsal region of the prosomere 2 was dissected from E13.5 mouse embryos and incubated with 0.05% Trypsin with 0.481 mM EDTA (Invitrogen) for 25 min at 37°C. Then, tissues were mildly triturated with a pipette. Dissociated cells (0.11×10^6 cells/cm^2) were seeded on approximately 80% confluent HEK293T cells expressing FLAG-tagged Linx plated on glass cover slips coated with 0.1 mg/ml poly-D-lysine (Sigma) and 10 ng/ml laminin (Invitrogen). Cells were cultured in Neurobasal media (Invitrogen) with 1 × B-27 supplement (Invitrogen), 2 mM L-glutamine, 10% fetal bovine serum, 50 U/ml penicillin, and 50 ng/ml streptomycin for 48 h. Then, cells were subjected to immunofluorescence staining with the class III β-tubulin (Tuj1) antibody. The longest axon of each neuron was measured after randomly selecting 50 neurons from each preparation. Results were compared to controls using a two-tailed Student's t-test. To express FLAG-tagged Linx in 293T cells, pFLAG-CMV1 Linx, which was designed to express a Linx (amino acids 20 to 745) fusion protein with an N-terminal FLAG epitope, was transfected with Lipofectamine 2000 (Invitrogen).

Supplementary Material

Refer to Web version on PubMed Central for supplementary material.

Acknowledgments

We thank Randal Hand and members of the Ginty lab for comments on the manuscript; Holly Wellington for ES cell work; Charles Hawkins and the Johns Hopkins Transgenic Facility for blastocyst injections; Kenneth Campbell for *Dlx5/6*-Cre mice; Noriko Hattori for technical assistance; and members of the Ginty laboratory for discussions and technical assistance throughout the course of this project. This research was supported by National Institutes of Health grant NS34814 (D.D.G.) and Grants-in-Aid for Scientific Research on Innovative Areas ("Brain Environment" 24111532 and "Neocortical Organization" 25123713) from the Ministry of Education, Science, Sports and Culture of Japan (K.M.). D.D.G. is an investigator of the Howard Hughes Medical Institute.

References

Arlotta P, Molyneaux BJ, Chen J, Inoue J, Kominami R, Macklis JD. Neuronal subtype-specific genes that control corticospinal motor neuron development in vivo. Neuron. 2005; 45:207–221. [PubMed: 15664173]

Bielle F, Marcos-Mondéjar P, Keita M, Mailhes C, Verney C, Nguyen Ba-Charvet K, Tessier-Lavigne M, López-Bendito G, Garel S. Slit2 activity in the migration of guidepost neurons shapes thalamic projections during development and evolution. Neuron. 2011; 69:1085–1098. [PubMed: 21435555]

Blakemore C, Molnár Z. Factors involved in the establishment of specific interconnections between thalamus and cerebral cortex. Cold Spring Harb Symp Quant Biol. 1990; 55:491–504. [PubMed: 2132833]

Chen Y, Magnani D, Theil T, Pratt T, Price DJ. Evidence that descending cortical axons are essential for thalamocortical axons to cross the pallial-subpallial boundary in the embryonic forebrain. PLoS One. 2012; 7:e33105. [PubMed: 22412988]

Deck M, Lokmane L, Chauvet S, Mailhes C, Keita M, Niquille M, Yoshida M, Yoshida Y, Lebrand C, Mann F, et al. Pathfinding of corticothalamic axons relies on a rendezvous with thalamic projections. Neuron. 2013; 77:472–484. [PubMed: 23395374]

Demyanenko GP, Riday TT, Tran TS, Dalal J, Darnell EP, Brennaman LH, Sakurai T, Grumet M, Philpot BD, Maness PF. NrCAM deletion causes topographic mistargeting of thalamocortical axons to the visual cortex and disrupts visual acuity. J Neurosci. 2011; 31:1545–1558. [PubMed: 21273439]

Dufour A, Seibt J, Passante L, Depaepe V, Ciossek T, Frisén J, Kullander K, Flanagan JG, Polleux F, Vanderhaeghen P. Area specificity and topography of thalamocortical projections are controlled by ephrin/Eph genes. Neuron. 2003; 39:453–465. [PubMed: 12895420]

Ferland RJ, Cherry TJ, Preware PO, Morrisey EE, Walsh CA. Characterization of Foxp2 and Foxp1 mRNA and protein in the developing and mature brain. J Comp Neurol. 2003; 460:266–279. [PubMed: 12687690]

Flanagan JG, Cheng HJ, Feldheim DA, Hattori M, Lu Q, Vanderhaeghen P. Alkaline phosphatase fusions of ligands or receptors as in situ probes for staining of cells, tissues, and embryos. Methods Enzymol. 2000; 327:19–35. [PubMed: 11044971]

Giger RJ, Urquhart ER, Gillespie SK, Levengood DV, Ginty DD, Kolodkin AL. Neuropilin-2 is a receptor for semaphorin IV: insight into the structural basis of receptor function and specificity. Neuron. 1998; 21:1079–1092. [PubMed: 9856463]

Gorski JA, Talley T, Qiu M, Puelles L, Rubenstein JL, Jones KR. Cortical excitatory neurons and glia, but not GABAergic neurons, are produced in the Emx1-expressing lineage. J Neurosci. 2002; 22:6309–6314. [PubMed: 12151506]

Hevner RF, Miyashita-Lin E, Rubenstein JL. Cortical and thalamic axon pathfinding defects in Tbr1, Gbx2, and Pax6 mutant mice: evidence that cortical and thalamic axons interact and guide each other. J Comp Neurol. 2002; 447:8–17. [PubMed: 11967891]

Leyva-Díaz E, López-Bendito G. In and out from the cortex: development of major forebrain connections. Neuroscience. 2013; 254:26–44. [PubMed: 24042037]

Liu P, Jenkins NA, Copeland NG. A highly efficient recombineering-based method for generating conditional knockout mutations. Genome Res. 2003; 13:476–484. [PubMed: 12618378]

López-Bendito G, Cautinat A, Sánchez JA, Bielle F, Flames N, Garratt AN, Talmage DA, Role LW, Charnay P, Marín O, Garel S. Tangential neuronal migration controls axon guidance: a role for neuregulin-1 in thalamocortical axon navigation. Cell. 2006; 125:127–142. [PubMed: 16615895]

López-Bendito G, Molnár Z. Thalamocortical development: how are we going to get there? Nat Rev Neurosci. 2003; 4:276–289. [PubMed: 12671644]

Mandai K, Guo T, St Hillaire C, Meabon JS, Kanning KC, Bothwell M, Ginty DD. LIG family receptor tyrosine kinase-associated proteins modulate growth factor signals during neural development. Neuron. 2009; 63:614–627. [PubMed: 19755105]

McConnell SK, Ghosh A, Shatz CJ. Subplate neurons pioneer the first axon pathway from the cerebral cortex. Science. 1989; 245:978–982. [PubMed: 2475909]

Métin C, Déleglise D, Serafini T, Kennedy TE, Tessier-Lavigne M. A role for netrin-1 in the guidance of cortical efferents. Development. 1997; 124:5063–5074. [PubMed: 9362464]

Métin C, Godement P. The ganglionic eminence may be an intermediate target for corticofugal and thalamocortical axons. J Neurosci. 1996; 16:3219–3235. [PubMed: 8627360]

Molnár Z, Adams R, Blakemore C. Mechanisms underlying the early establishment of thalamocortical connections in the rat. J Neurosci. 1998a; 18:5723–5745. [PubMed: 9671663]

Molnár Z, Adams R, Goffinet AM, Blakemore C. The role of the first postmitotic cortical cells in the development of thalamocortical innervation in the reeler mouse. J Neurosci. 1998b; 18:5746–5765. [PubMed: 9671664]

Molnár Z, Garel S, López-Bendito G, Maness P, Price DJ. Mechanisms controlling the guidance of thalamocortical axons through the embryonic forebrain. Eur J Neurosci. 2012; 35:1573–1585. [PubMed: 22607003]

Puelles L, Rubenstein JL. Forebrain gene expression domains and the evolving prosomeric model. Trends Neurosci. 2003; 26:469–476. [PubMed: 12948657]

Robichaux MA, Chenaux G, Ho HY, Soskis MJ, Dravis C, Kwan KY, Sestan N, Greenberg ME, Henkemeyer M, Cowan CW. EphB receptor forward signaling regulates area-specific reciprocal thalamic and cortical axon pathfinding. Proc Natl Acad Sci U S A. 2014; 111:2188–2193. [PubMed: 24453220]

Stenman J, Toresson H, Campbell K. Identification of two distinct progenitor populations in the lateral ganglionic eminence: implications for striatal and olfactory bulb neurogenesis. J Neurosci. 2003; 23:167–174. [PubMed: 12514213]

Stoykova A, Fritsch R, Walther C, Gruss P. Forebrain patterning defects in Small eye mutant mice. Development. 1996; 122:3453–3465. [PubMed: 8951061]

Suzuki-Hirano A, Ogawa M, Kataoka A, Yoshida AC, Itoh D, Ueno M, Blackshaw S, Shimogori T. Dynamic spatiotemporal gene expression in embryonic mouse thalamus. J Comp Neurol. 2011; 519:528–543. [PubMed: 21192082]

Tuttle R, Nakagawa Y, Johnson JE, O'Leary DD. Defects in thalamocortical axon pathfinding correlate with altered cell domains in Mash-1-deficient mice. Development. 1999; 126:1903–1916. [PubMed: 10101124]

Uemura M, Nakao S, Suzuki ST, Takeichi M, Hirano S. OL-Protocadherin is essential for growth of striatal axons and thalamocortical projections. Nat Neurosci. 2007; 10:1151–1159. [PubMed: 17721516]

Wang Y, Thekdi N, Smallwood PM, Macke JP, Nathans J. Frizzled-3 is required for the development of major fiber tracts in the rostral CNS. J Neurosci. 2002; 22:8563–8573. [PubMed: 12351730]

Wright AG, Demyanenko GP, Powell A, Schachner M, Enriquez-Barreto L, Tran TS, Polleux F, Maness PF. Close homolog of L1 and neuropilin 1 mediate guidance of thalamocortical axons at the ventral telencephalon. J Neurosci. 2007; 27:13667–13679. [PubMed: 18077678]

Zhou L, Bar I, Achouri Y, Campbell K, De Backer O, Hebert JM, Jones K, Kessaris N, de Rouvroit CL, O'Leary D, et al. Early forebrain wiring: genetic dissection using conditional Celsr3 mutant mice. Science. 2008; 320:946–949. [PubMed: 18487195]

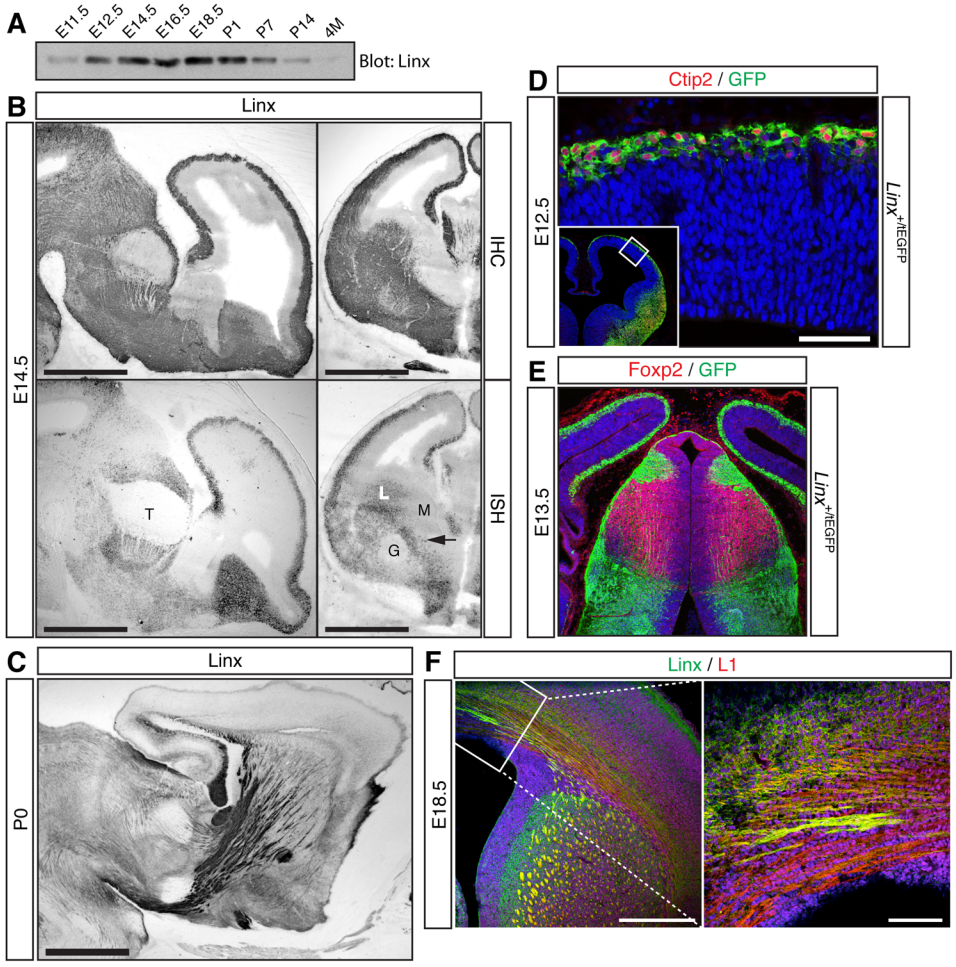

Figure 1. Expression of Linx in the developing brain

(A) Western blot probed with anti-Linx. An aliquot of 40 μg protein of brain homogenatewas loaded into each lane. E: embryonic day, P: postnatal day, M: month. (B)Immunohistochemistry (IHC) with anti-Linx and *in situ* hybridization (ISH) probed for*Linx*. Sagittal (left) and coronal (right) sections of wild-type mouse brain at E14.5 areshown. Adjacent sections were used for analyses. The specificity of anti-Linx used for theseIHC experiments is documented in findings shown in Figure S1 and elsewhere (Mandai etal., 2009). Arrow, lateral ganglionic eminence (LGE)-derived corridor; L, LGE; M, medialganglionic eminence; T, thalamus; G, globus pallidus. (C) A sagittal section of P0 wild-typemouse brain stained with anti-Linx. (D) Coronal sections of the developing neocortex of a*Linx*$^{+/tEGFP}$ embryo stained with GFP (green) and Ctip2 (red) antibodies and counterstainedwith TO-PRO-3 (blue) at E12.5. The boxed area shown in the inset is magnified. (E) Acoronal section of the developing thalamus of a *Linx*$^{+/tEGFP}$ embryo stained with GFP(green) and Foxp2 (red) antibodies and counterstained with TO-PRO-3 (blue) at E13.5. (F)Coronal sections of the neocortex of an E18.5 wild-type embryo stained with Linx (green)and L1 (red) antibodies and counterstained with TO-PRO-3 (blue).

Bars, 1.0 mm (B and C), 50 μm (D), 0.4 mm (E and F left) and 0.1 mm (F right). These results are representative of three independent experiments.

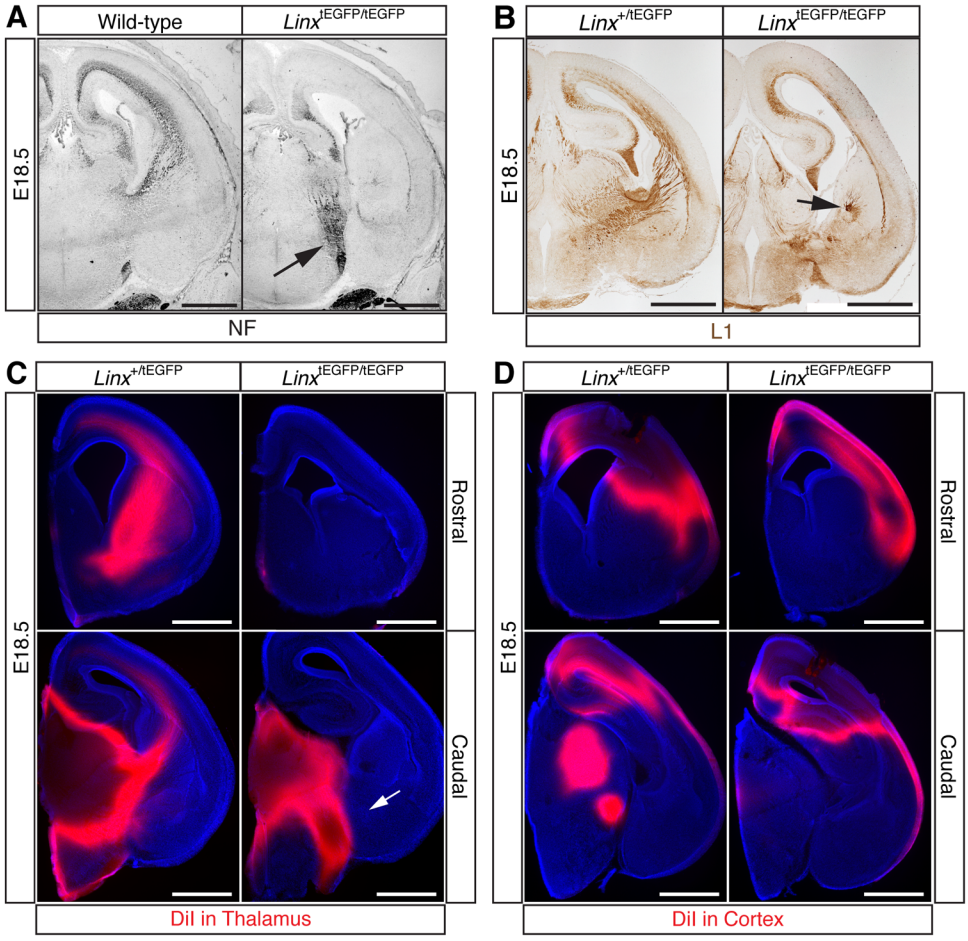

Figure 2. Linx is required for internal capsule formation

Coronal sections of E18.5 brains. Immunostaining with anti-Neurofilament (A) and anti-L1 (B) in control (wild-type in A and *Linx*$^{+/tEGFP}$ in B) and *Linx*$^{tEGFP/tEGFP}$ mice, and tracing of axon tracts that connect the neocortex and thalamus in *Linx*$^{+/tEGFP}$ (control) and *Linx*$^{tEGFP/tEGFP}$ mice with DiI crystals inserted into the thalamus (C) or somatosensory cortex (D). Sections were counterstained with Hoechst 33258 in C and D. Arrows, misrouted thalamocortical projections (A and C) and remnants of the descending component of the internal capsule (B). Bars, 1 mm. These results are representative of at least eight (A) and four independent experiments (B-D). See also Figure S2.

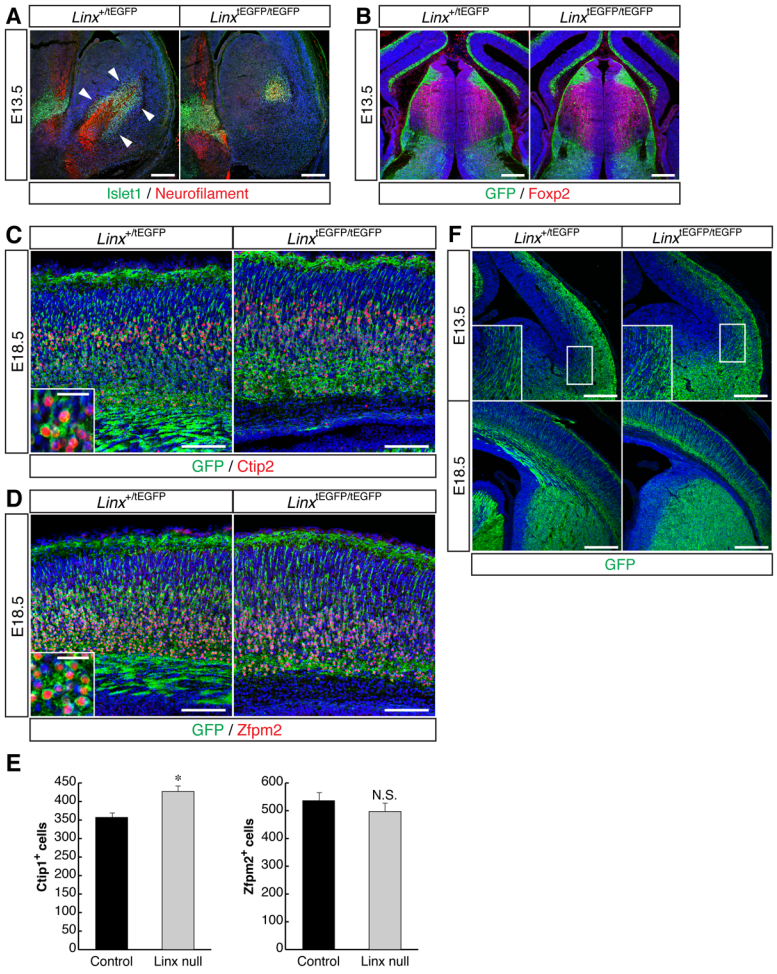

Figure 3. Linx mediates thalamocortical and corticofugal axon guidance

(A-D) Immunostaining analyses of brains of *Linx*$^{+/tEGFP}$ (control) and *Linx*$^{tEGFP/tEGFP}$ embryos. (A) Coronal sections of the ventral forebrain immunostained with anti-Islet1 (green), anti-Neurofilament (red), and TO-PRO-3 (blue) at E13.5. Arrowheads flank the LGE-derived corridor. (B) Coronal sections of the thalamus immunostained with anti-GFP (green), anti-Foxp2 (red), and TO-PRO-3 (blue) at E13.5. (C and D) Coronal sections of the somatosensory cortices immunostained with anti-GFP (green), anti-Ctip2 (C) or anti-Zfpm2 (D) (red), and TO-PRO-3 (blue) at E18.5. (E) Quantification for results shown in C and D. Neurons positive for Ctip2 or Zfpm2 were counted in a square field of view, 460.7 μm on a side, in the neocortex using three sections per embryo (a total of nine sections from three embryos for each group). Shown are means +/- s.e.m. Statistical analysis was performed using two-tailed Student's t-test. *, $p=5.7\times10^{-3}$. N.S., not significant. (F) Coronal sections of forebrains immunostained with anti-GFP (green) and TO-PRO-3 (blue) in *Linx*$^{+/tEGFP}$ (control) and *Linx*$^{tEGFP/tEGFP}$ embryos at E13.5 or E18.5. Insets, magnified images of the boxed areas. Bars, 0.2 mm (A, B, and F), 0.1 mm (C and D), and 20 μm (insets in C and D). Results shown are representative of at least three independent experiments. See also Figure S3.

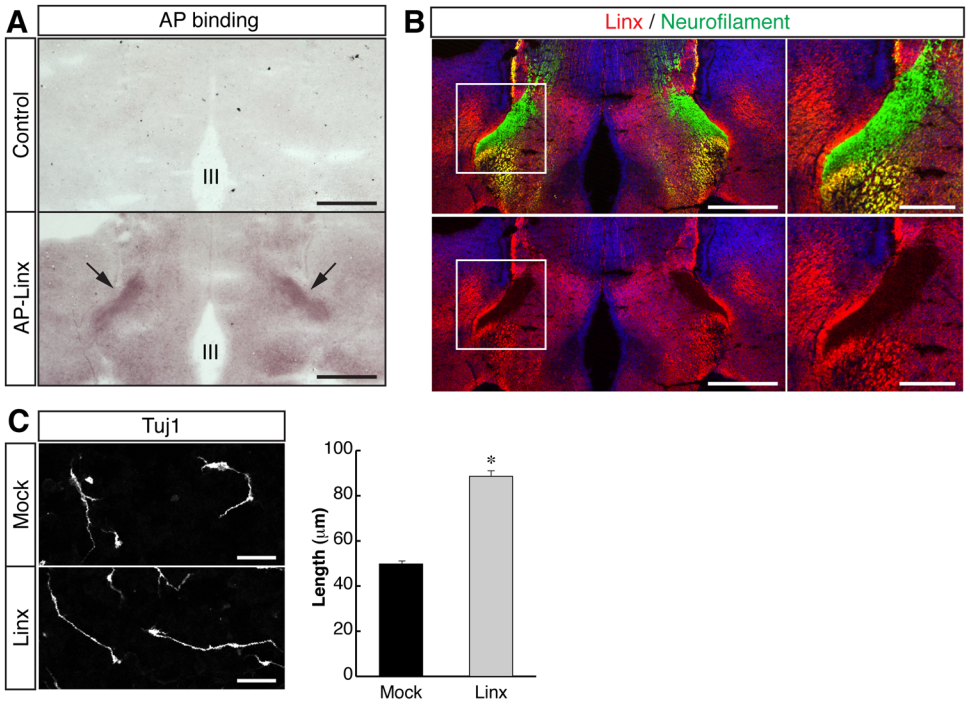

Figure 4. Linx binds to thalamocortical axons in vivo and promotes thalamic neuron axon extension in vitro

(A) Adjacent coronal sections of an E14.5 wild-type brain, incubated with alkaline-phosphatase (AP) tagged ectodomain of Linx (AP-Linx) or AP alone as a control. Binding sites of the AP ligands are detected with AP color reaction. Arrows, thalamocortical projections. III, the third ventricle. These results are representative data from three independent experiments. (B) Immunostaining with anti-Neurofilament (green), anti-Linx (red), and TO-PRO-3 (blue). After the AP color reaction, specimens were stained using antibodies. Superimposed images of all three channels are shown in the upper row, while the red and blue channels are shown in the lower row. Boxed regions are highlighted in the right column. Bars, 0.5 mm (A and B (left)) and 0.2 mm (B (right)). (C) In vitro neurite outgrowth of dissociated thalamic neurons. Dissociated thalamic neurons obtained from E13.5 wild-type embryos were cultured for 48 h on monolayers of 293T cells expressing FLAG-tagged Linx or mock-transfected 293T cells. Axons were stained with anti-class III β-tubulin (Tuj1) (left) and the average length of axons is presented (right). Bars, 50 μm. From 3 sets of independent experiments, 50 neurons per experiment (for a total of 150 neurons for each group) were randomly selected and analyzed. Statistical analysis was performed using two-tailed Student's t-test. *, $p=1.6\times10^{-36}$; Shown are means +/- s.e.m.

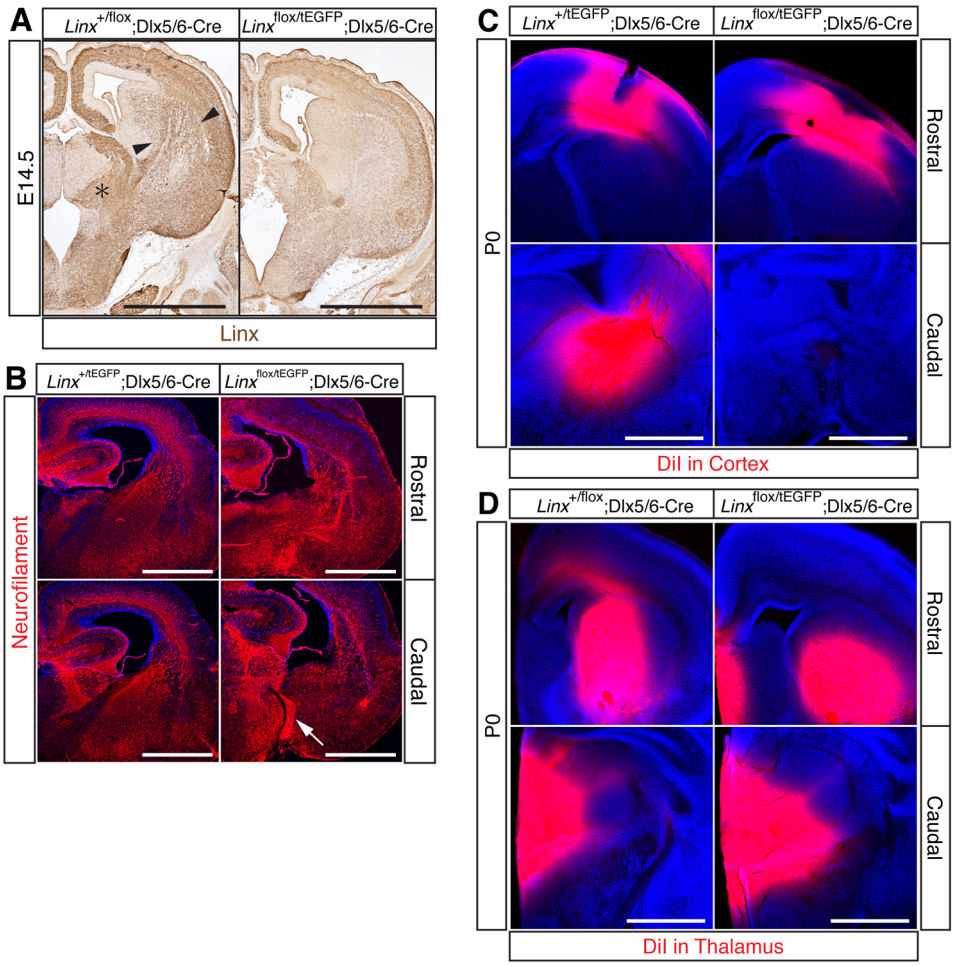

Figure 5. Linx functions in the ventral forebrain to promote axonal projections through the DTB and for internal capsule formation

(A) Coronal sections of *Linx*$^{+/flox}$;*Dlx5/6*-Cre (control) and *Linx*$^{tEGFP/flox}$;*Dlx5/6*-Cre brains stained with anti-Linx at E14.5. Asterisk, the prethalamus. Arrowheads flank the LGE. (B-D) Coronal sections of *Linx*$^{+/tEGFP}$;*Dlx5/6*-Cre or *Linx*$^{+/flox}$;*Dlx5/6*-Cre (control) and *Linx*$^{tEGFP/flox}$;*Dlx5/6*-Cre forebrains at P0. (B) Staining with anti-Neurofilament (red) and TO-PRO-3 (blue). Rostral and caudal parts of the internal capsule are shown. Arrow, misrouted thalamocortical projections. (C and D) Tracing of axon tracts that connect the neocortex and thalamus by placing DiI crystals into the somatosensory cortex (C) or thalamus (D). Note that for experiments shown in D, larger DiI crystals were used than for experiments shown in C in order to enhance visualization of the distal thalamocortical projections into the neocortex. Therefore, anterogradely labeled thalamocortical axons that have misprojected into the ventral forebrain are obscured due to heavy DiI labeling; These ventral misprojections of *Linx*$^{tEGFP/flox}$;*Dlx5/6*-Cre mice are observed in immunohistochemistry experiments shown in panels A and B. Sections were counterstained with Hoechst 33258. Bars, 1.0 mm. The experiments in A and B were done three times using three mice, with similar findings. The experiments in C and D were done four times using four mice, with similar findings. See also Figure S4.

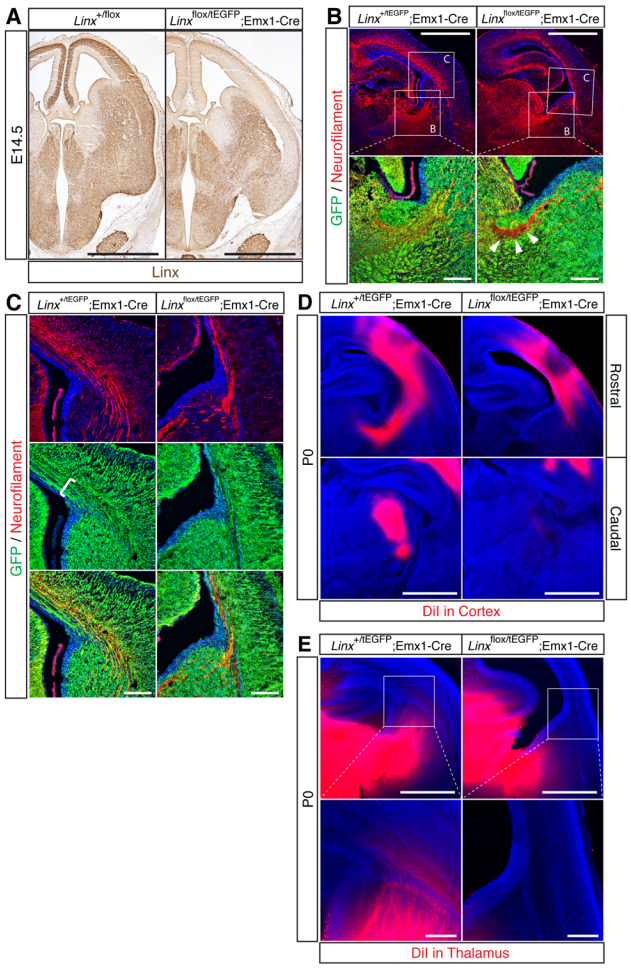

Figure 6. Linx functions in the cortical neurons to promote axonal projections through the PSPB and for internal capsule formation

(A) Coronal sections of *Linx*$^{+/flox}$ (control) and *Linx*$^{tEGFP/flox}$;*Emx1*-Cre brains stained with anti-Linx at E14.5. (B-E) Coronal sections of *Linx*$^{+/tEGFP}$;*Emx1*-Cre (control) and *Linx*$^{tEGFP/flox}$;*Emx1*-Cre brains at P0. (B and C) Staining with anti-GFP (green), anti-Neurofilament (red), and TO-PRO-3 (blue). The boxed areas are magnified in the lower panels in B or C. (B) Note that the main trunk of the mutant internal capsule (labeled with arrowheads) is hypoplastic and devoid of GFP signal, and that axons in the mutant neocortex are poorly stained with anti-Neurofilament. (C) Magnified images of the tissues near the PSPB shown in (B). Note that few corticofugal and thalamocortical axons cross the PSPB in the mutant. Bracket, corticofugal axons visualized with GFP signals from the *Linx*^{tEGFP} allele. (D and E) Tracing of axon tracts that connect the neocortex and thalamus by placing DiI crystals into the somatosensory cortex (D) or thalamus (E). Sections were counterstained with Hoechst 33258. Bars, 1mm (A, B upper, D, E upper) and 0.2 mm (B lower, C, and E lower). The experiments in A, B, and C were done three times using three mice, with similar findings. The experiments in D and E were done four times using four mice, with similar findings. See also Figure S4.

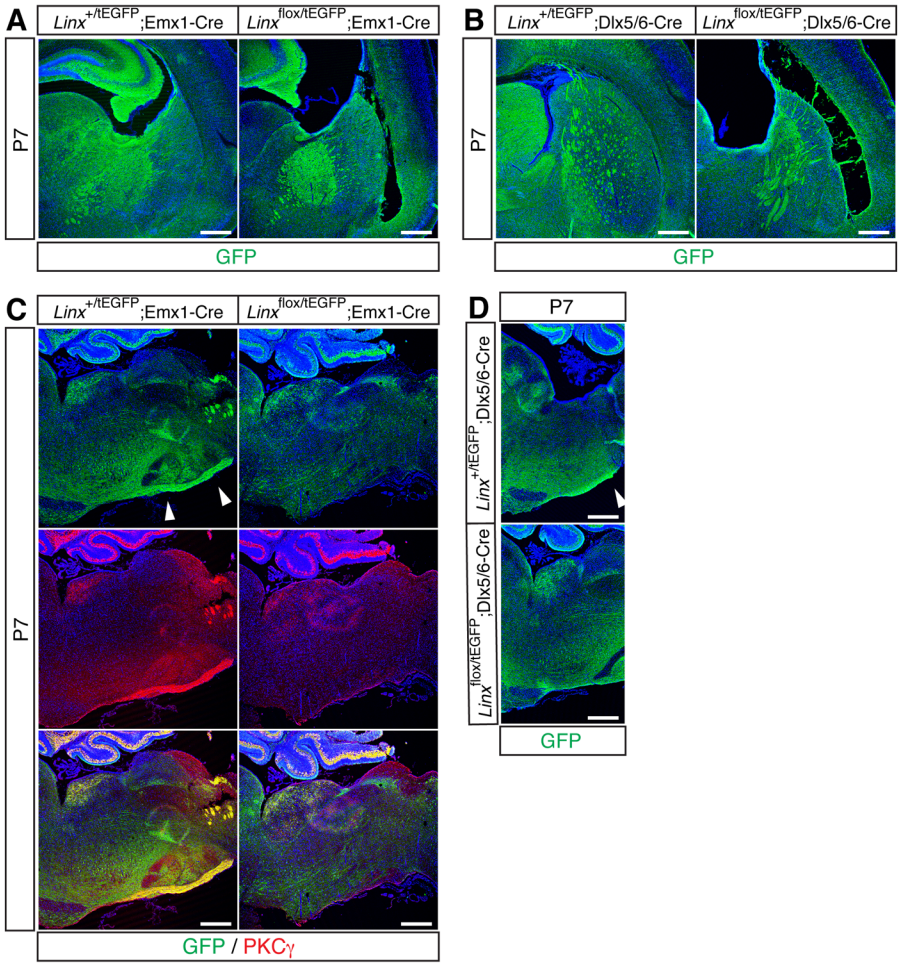

Figure 7. Defects in the internal capsule and corticospinal tract in P7 *Linx* mutant mice

(A) Coronal sections of *Linx*$^{+/tEGFP}$;*Emx1*-Cre (control) and *Linx*$^{tEGFP/flox}$;*Emx1*-Cre ventral forebrains stained with anti-GFP and DAPI (blue). (B) Coronal sections of *Linx*$^{+/tEGFP}$;*Dlx5/6*-Cre (control) and *Linx*$^{tEGFP/flox}$;*Dlx5/6*-Cre ventral forebrains stained with anti-GFP and DAPI (blue). (C) Sagittal sections of *Linx*$^{+/tEGFP}$;*Emx1*-Cre (control) and *Linx*$^{tEGFP/flox}$;*Emx1*-Cre brain stems stained with anti-GFP (green), anti-PKCγ (green) and DAPI (blue). (D) Sagittal sections of *Linx*$^{+/tEGFP}$;*Dlx5/6*-Cre (control) and *Linx*$^{tEGFP/flox}$;*Dlx5/6*-Cre brain stems stained with anti-GFP and DAPI (blue). Arrowheads, the corticospinal tract (C and D). Bars, 0.4 mm. These experiments were done three times using three mice, with similar findings. See also Figure S4.